Phase behaviour of fluids confined between chemically decorated substrates

2001 J. Phys.: Condens. Matter 13 4697

(http://iopscience.iop.org/0953-8984/13/21/305)

INSTITUTE OF PHYSICS PUBLISHING JOURNAL OF PHYSICS: CONDENSED MATTER

J. Phys.: Condens. Matter **13** (2001) 4697–4714 www.iop.org/Journals/cm PII: S0953-8984(01)19620-7

Phase behaviour of fluids confined between chemically decorated substrates

Henry Bock, Dennis J Diestler[1] and Martin Schoen[2]

Iwan-N-Stranski-Institut für Physikalische und Theoretische Chemie, Sekretariat TC7, Technische Universität Berlin, Straße des 17 Juni 124, D-10623 Berlin, Germany

E-mail: henry@terra.chem.tu-berlin.de (H Bock), ddiestler1@unl.edu (D J Diestler) and martin@terra.chem.tu-berlin.de (M Schoen)

Received 29 November 2000

Abstract

The phase behaviour of a lattice gas confined between two identical plane-parallel substrates decorated with weakly and strongly adsorbing stripes that alternate periodically in one transverse direction is explored within mean-field theory. It is shown that in the limit of zero temperature ($T = 0$), the mean-field approximation becomes exact. A modular approach is used to enumerate the possible structural types of phases (morphologies) that can exist at $T = 0$. Analytic expressions for the grand potentials associated with the morphologies can be obtained and used to determine the exact phase diagram at $T = 0$. In addition to the known 'gas', 'liquid', and 'bridge' phases, new 'vesicle', 'droplet', and 'layered' morphologies arise, which were overlooked in previous studies of this model. These $T = 0$ morphologies are taken as trial starting solutions in an iterative numerical procedure for solving the mean-field equations for $T > 0$. The complete phase diagram is thus obtained and its structure is studied as a function of the relative strength of 'strong' and 'weak' stripes. A key finding is that the number of possible morphologies increases rapidly with the geometrical complexity of the decoration of the substrate. The implications for the determination of phase diagrams for very complex confined systems (e.g. fluids in random porous media) are discussed.

1. Introduction

The emergence of a number of novel techniques in materials science, such as lithography [1,2], wet chemical etching [3], and microcontact printing [4–6], has permitted the fabrication of solid substrates with stable, precisely characterized surface structures on length scales ranging from microns to nanometres. Such chemically decorated substrates play an important rôle in a

[1] Guest scientist of Sonderforschungsbereich 448 'Mesoskopisch strukturierte Verbundsysteme'; permanent address: Department of Agronomy and Horticulture, University of Nebraska–Lincoln, Lincoln NE 68583-0915, USA.

[2] Author to whom any correspondence should be addressed.

0953-8984/01/214697+18$30.00

variety of contexts. One of these is the field of microfluidics [7,8] where the wettability of the substrate surface is modified so as to create chemical lanes along which nanoscopic portions of fluid may be transported from one site to another, where, for example, they may undergo chemical reaction with another fluid similarly transported from yet a third site. It is conceivable that substrates endowed with an integrated network of chemical lanes could function as minute chemical factories, or chemical 'chips' [8]. Another realization of a chemically decorated substrate is the 'Janus bead', a spherical colloidal particle with hydrophilic and hydrophobic hemispheres separated by a sharply defined equator [9, 10]. The amphiphilic Janus beads can be used to stabilize oil–water interfaces [9].

The potential importance of structured substrates in the manipulation of fluids at very short length scales has spurred a parallel theoretical interest in the behaviour of such confined fluids. Fluids constrained by chemically decorated substrates have an especial curiosity on account of their expected complex phase diagrams. A prototypical case consists of fluid confined between identical plane-parallel substrates, each decorated with weakly and strongly attractive stripes that alternate periodically in one direction (say x) parallel with the interface. The stripes are infinite in the other transverse direction (y). Röcken and co-workers [11,12] first demonstrated the existence of a 'bridge' phase in this type of system. In more recent work we have explored the properties of the bridge phase in some detail [13–17]. The bridge phase, a new type of phase distinct from the gas and liquid phases known to form between substrates that are strictly homogeneous in transverse dimensions, comprises high- and low-density regions separated by an interface perpendicular to the substrates. The interface resembles the one at bulk liquid–gas coexistence [13]. Thus, bridge phases are inhomogeneous in the direction perpendicular to the interface. In the direction perpendicular to the substrate plane the high(er)-density portion of a bridge phase is stratified; that is, molecules arrange themselves in individual layers parallel with that plane. Coexistence between gaslike, liquidlike, and bridge phases depends crucially on the chemical corrugation of the decorated substrate, that is on the relative widths of the weakly and strongly adsorbing stripes [14, 15]. By virtue of the geometry of the substrates and the inhomogeneity of bridge phases, the latter can be subjected to shear strains by misaligning the former [17].

However, as we shall demonstrate below, the phase behaviour of the prototypal model is considerably richer than has been realized in any of the preceding studies [11–17]. For example, lanes of liquid ('droplets') may form along the attractive stripes, which are thermodynamically stable over a wide temperature range. Structurally these lanes are akin to those observed in [18, 19], even though the latter exist on μm (rather than nm) length scales. Yet another phase may be described as 'vesicular', where low-density tunnels over the weak stripes are immersed in high(er)-density fluid. In addition, one encounters layering transitions depending on the relative difference between the strength of the attraction of weak and strong stripes.

The question that we address here concerns the completeness of the phase diagram. That is, given a specification of the chemical decoration, can we determine all the possible structural types of phase (to which we shall refer subsequently as 'morphologies') of the confined fluid that can exist (or coexist)? We have sought a partial answer to this question by exploring the phase behaviour of the chemically striped prototype described above within the framework of the lattice gas. Here we follow the seminal paper by Pandit *et al* [20], emphasizing the limit of zero temperature ($T = 0$), where the above problem can be investigated analytically. From the limit $T = 0$ we deduce suitable starting conditions for a subsequent mean-field treatment for $T > 0$.

In section 2 we describe the lattice-gas model for confined fluids (of which the prototype is a special case) and derive an explicit expression for the *exact* grand potential at $T = 0$. We present a mean-field treatment of the model in section 3, demonstrating that the mean-field

grand potential becomes exact in the limit of vanishing temperature. Section 4 is devoted to the enumeration of the possible morphologies (i.e., morphologically distinct phases) of the prototype at $T = 0$. We also show how the phase equilibria among morphologies can be determined analytically in this limit. Section 5 presents the results (e.g., phase diagrams) of numerical solutions of the mean-field equations for $T > 0$. Section 6 concludes the paper with a summary of our findings and a discussion of their implications.

2. Lattice model

We consider a fluid made up of structureless (spherically symmetric) molecules, the positions of which are constrained to the sites of an $n_x \times n_y \times n_z$ simple cubic lattice, with lattice constant ℓ infinitesimally larger than the molecular diameter. Any site can be occupied by at most a single molecule. This restriction reflects the infinite hard-core repulsion between molecules. The intermolecular interaction is described by a square-well potential, where the depth and width of the attractive well are $\epsilon_{\rm ff}$ and ℓ, respectively. This is equivalent to taking only nearest-neighbour interactions into account. We also assume that the fluid is confined in the z-direction between two plane-parallel substrates. The interaction of a molecule at site i with the substrates is represented by the potential energy Φ_i. Thus, the total potential energy of the lattice gas in a given configuration can be written as

$$U = -\frac{\epsilon_{\rm ff}}{2}\sum_{i=1}^{\mathcal{N}}\sum_{j\neq i}^{\nu(i)} s_i s_j + \sum_{i=1}^{\mathcal{N}} \Phi_i s_i \tag{2.1}$$

where s_i stands for the occupation number of site i, which can be 0 (empty site) or 1 (occupied site), $\mathcal{N} = n_x n_y n_z$ is the number of lattice sites, and $\nu(i)$ is the number of nearest neighbours ($\nu(i) = 5$ or 6, depending on the location of site i).

The grand partition function for the confined lattice gas can be expressed as

$$\Xi = \sum_{\boldsymbol{s}} \exp\left\{-\beta\left[-\frac{\epsilon_{\rm ff}}{2}\sum_{i=1}^{\mathcal{N}}\sum_{j\neq i}^{\nu(i)} s_i s_j + \sum_{i=1}^{\mathcal{N}}\Phi_i s_i - \mu\sum_{i=1}^{\mathcal{N}} s_i\right]\right\} \tag{2.2}$$

where the sum is over all *sets* of occupation numbers $\boldsymbol{s} = \{s_1, s_2, \ldots, s_{\mathcal{N}}\}$. In equation (2.2) $\beta = (k_{\rm B}T)^{-1}$ and μ is the chemical potential. We note that this model has been previously employed in studies of wetting of homogeneous walls [21–23] and of adsorption in slit pores with chemically heterogeneous substrates [15–17].

The grand partition function given in (2.2) can be rewritten as

$$\Xi = \exp[-\beta t(\boldsymbol{s}_0)]\left(1 + \sum_{\boldsymbol{s}\neq\boldsymbol{s}_0}\exp\{-\beta[t(\boldsymbol{s}) - t(\boldsymbol{s}_0)]\}\right) \tag{2.3}$$

where

$$t(\boldsymbol{s}) \equiv -\frac{\epsilon_{\rm ff}}{2}\sum_{i=1}^{\mathcal{N}}\sum_{j}^{\nu(i)} s_i s_j + \sum_i [\Phi_i - \mu]s_i \tag{2.4}$$

and we suppose that the set of occupation numbers $\boldsymbol{s}_0$ is the one for which $t(\boldsymbol{s})$ is minimum, i.e., $t(\boldsymbol{s}) > t(\boldsymbol{s}_0)$ for all $\boldsymbol{s} \neq \boldsymbol{s}_0$. From (2.3) we obtain for the grand potential Ω

$$\Omega = -\beta^{-1}\ln\Xi = t(\boldsymbol{s}_0) - \beta^{-1}\ln\left\{1 + \sum_{\boldsymbol{s}\neq\boldsymbol{s}_0}\exp(-\beta[t(\boldsymbol{s}) - t(\boldsymbol{s}_0)])\right\}. \tag{2.5}$$

As $T \to 0$, the logarithmic term in (2.5) vanishes, leaving

$$\Omega = t(\boldsymbol{s}_0) = -\frac{\epsilon_{\rm ff}}{2}\sum_{i=1}^{\mathcal{N}}\sum_{j\neq i}^{\nu(i)} s_{i0}s_{j0} + \sum_{i=1}^{\mathcal{N}}[\Phi_i - \mu]s_{i0}. \tag{2.6}$$

3. Mean-field theory

3.1. The grand potential

To obtain a closed expression for the grand potential of a lattice gas at non-zero temperature we utilize the classical version of the Bogoliubov theorem [24, 25], which states

$$\Omega \leqslant \Omega^{(0)} + \langle U - U^{(0)} \rangle_0 \tag{3.1}$$

where Ω is the *exact* grand potential for the system of interest whose configurational energy is U and $\Omega^{(0)}$ is the (exact) grand potential for a reference (unperturbed) system whose configurational energy is $U^{(0)}$. The 'correction' $\langle U - U^{(0)} \rangle_0$ is determined as a grand canonical ensemble average over the states of the reference system.

In the present case of the nearest-neighbour lattice-gas model, U is given by (2.1). For the reference system we take

$$U^{(0)} = \sum_{i=1}^{\mathcal{N}} \Psi_i s_i \tag{3.2}$$

where Ψ_i is an *a priori* unknown external reference potential to be determined by minimizing the right-hand side of (3.1). From (2.2) we have by analogy

$$\begin{aligned} \Xi^{(0)} = \sum_s \exp\left\{-\beta\left[\sum_i (\Psi_i - \mu) s_i\right]\right\} &= \prod_{i=1}^{\mathcal{N}} \sum_{s_i=0}^{1} \exp\{-\beta(\Psi_i - \mu) s_i\} \\ &= \prod_{i=1}^{\mathcal{N}} \{1 + \exp[-\beta(\Psi_i - \mu)]\} \end{aligned} \tag{3.3}$$

where the second equality follows from the independence of the s_i. The correction is given by

$$\langle U - U^{(0)} \rangle_0 = -\frac{\epsilon_{\mathrm{ff}}}{2} \sum_{i=1}^{\mathcal{N}} \sum_{j \neq i}^{\nu(i)} \rho_i \rho_j + \sum_{i=1}^{\mathcal{N}} (\Phi_i - \Psi_i) \rho_i \tag{3.4}$$

where $\rho_i \equiv \langle s_i \rangle_0$ is the mean occupation number (equivalent to the dimensionless local density in units of ℓ^{-3}). It is given in terms of the external reference potential by the relation

$$\rho_i = \frac{1}{1 + \exp[\beta(\Psi_i - \mu)]} \tag{3.5}$$

which, when combined with (3.1) and (3.4), leads to

$$\Omega \leqslant \Omega[\boldsymbol{\rho}] \equiv \beta^{-1} \sum_{i=1}^{\mathcal{N}} [\rho_i \ln \rho_i + (1 - \rho_i) \ln(1 - \rho_i)] - \frac{\epsilon_{\mathrm{ff}}}{2} \sum_{i=1}^{\mathcal{N}} \sum_{j \neq i}^{\nu(i)} \rho_i \rho_j + \sum_{i=1}^{\mathcal{N}} (\Phi_i - \mu) \rho_i \tag{3.6}$$

where $\Omega[\boldsymbol{\rho}]$ stands for the functional of the unknown densities on the right-hand side of (3.6). These and the best estimate of Ω are determined by minimizing $\Omega[\boldsymbol{\rho}]$, which is an upper bound on the exact grand potential. That is, we require

$$\frac{\delta \Omega[\boldsymbol{\rho}]}{\delta \rho_i} = 0 \qquad i = 1, \ldots, \mathcal{N}. \tag{3.7}$$

From (3.6) and (3.7), we obtain

$$\beta^{-1} \ln \frac{\rho_i}{1 - \rho_i} - \epsilon_{\mathrm{ff}} \sum_{j \neq i}^{\nu(i)} \rho_j + \Phi_i - \mu = 0 \qquad i = 1, \ldots, \mathcal{N}. \tag{3.8}$$

These coupled transcendental equations are identical with (A6) in [17] and can be solved numerically as detailed in this latter work.

3.2. The limit $T = 0$

In the limit of vanishing temperature, the mean-field treatment becomes exact. To demonstrate this we begin by examining the bulk system ($\Phi \equiv 0$), for which all ρ_i are equal by symmetry. Equation (3.8) then simplifies to

$$\beta^{-1} \ln \frac{\rho}{1-\rho} - 6\epsilon_{\rm ff}\rho - \mu = 0 \tag{3.9}$$

where $\nu(i) = 6$. In the customary dimensionless units (distance in units of ℓ, energy in units of $\epsilon_{\rm ff}$, temperature in units of $\epsilon_{\rm ff}/k_{\rm B}$), equation (3.9) can be recast as

$$\rho = \frac{1}{6}(Tx - \mu) \tag{3.10}$$

where we have introduced the definition of x:

$$\rho =: \frac{1}{1+\exp(-x)}. \tag{3.11}$$

Plotting ρ and $(Tx-\mu)/6$ versus x for the case $T < T_{\rm c} = \frac{3}{2}$ and $\mu = \mu_{\rm c} = -3$ (where $T_{\rm c}$ and $\mu_{\rm c}$ are the temperature and chemical potential at the bulk critical point), we find that (3.10) has three real roots $-x_0$, 0, and x_0 corresponding to the densities $1-\rho(x_0)$, $\frac{1}{2}$, and $\rho(x_0)$, respectively. Evaluating the second derivative of Ω with respect to ρ for the solution $\rho = \frac{1}{2}$, we obtain

$$\left.\frac{\partial^2\Omega(\rho)}{\partial\rho^2}\right|_{\rho=1/2} = \left.\frac{T}{\rho(1-\rho)}\right|_{\rho=1/2} - 6 = 4T - 6 \tag{3.12}$$

which is negative for all $T < T_{\rm c}$. Hence Ω has a maximum at $\rho = \frac{1}{2}$, which corresponds to an unstable thermodynamic state. The remaining solutions are minima and, in the light of the symmetry inherent in the expression for Ω (see (3.6)) when $\mu = \mu_{\rm c}$, it is clear that $\Omega[\rho(x_0)]$ and $\Omega[1-\rho(x_0)]$ are the equal values of the grand potential of coexisting 'gas' and 'liquid' phases. Furthermore, it is clear from (3.11) that in the limit $T = 0$ ($x_0 = \infty$),

$$\lim_{x_0\to\infty} \rho(x_0) = \lim_{x_0\to\infty} (1+{\rm e}^{-x_0})^{-1} = 1$$

and therefore $1-\rho(x_0) = 0$. By a similar analysis we obtain for the limiting ($T = 0$) stable solutions of equation (3.10) for $\mu > \mu_{\rm c}$ and $\mu < \mu_{\rm c}$ the respective values $\rho = 1$ (liquid) and $\rho = 0$ (gas). We conclude that, regardless of the value of the chemical potential, the only stable solutions of (3.10) are these two, respectively corresponding to the completely filled and completely empty lattice. This is precisely the conclusion reached from the exact limiting expression (2.6) for the bulk system:

$$\Omega_0 = -\mathcal{N}(3s_0^2 + \mu s_0). \tag{3.13}$$

We thus arrive at the gratifying result that, for the bulk system, the mean-field approximation agrees with the exact result at $T = 0$.

The above reasoning can be extended to the situation of primary interest here: the fluid is constrained in one dimension (z) by plane-parallel substrates that are chemically decorated with weakly and strongly adsorbing stripes that alternate periodically in the x-direction, so the external potential depends only on x and z (see figure 1). Thus, for given values of x and z the occupation numbers do not vary with the y-coordinate of the lattice site. That is, by symmetry all densities ρ_i along lines parallel with the y-axis are equal. Thus, using (3.8) we can write for a particular site i

$$\beta^{-1} \ln \frac{\rho_i}{1-\rho_i} - 2\epsilon_{\rm ff}\rho_i - \epsilon_{\rm ff}\sum_{j=1}\rho_j + \Phi_i - \mu = 0 \tag{3.14}$$

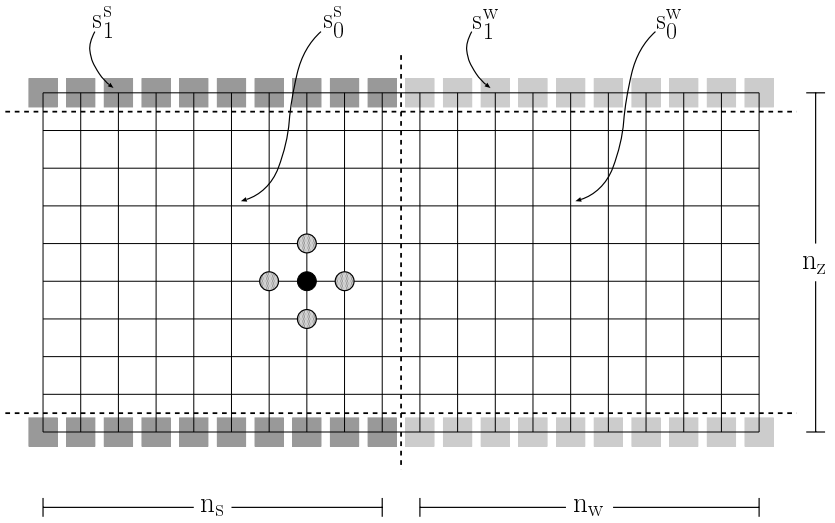

Figure 1. A schematic diagram of the prototypal model: cubic lattice gas confined between substrates consisting of strongly attractive stripes alternating periodically with weakly attractive ones. The dashed lines demarcate the four types of region (slabs) of the 'heterogeneous' module: central slabs (0) in weak (w) and strong (s) 'homogeneous' modules; outer slabs (1) in weak (w) and strong (s) 'homogeneous' modules. A molecule in the central region (black circle) interacts with its six nearest neighbours (the four in the x–z plane are depicted as grey circles; the two in the y-direction are not shown). Sites at which a molecules is subject to the strong attractive substrate ($\Phi_i = -\epsilon_{\rm fs}$) are indicated by dark grey squares; those at which a molecule is subject to the weak attractive substrate ($\Phi_i = -\epsilon_{\rm fw}$) are denoted by light grey squares.

where the factor of 2 comes from the two neighbours in the y-direction and the ρ_j are the (*a priori* unknown) densities of the four (or three) nearest-neighbour sites in the x–z plane. Using the definition of x given in (3.11), we can rewrite (3.14) in dimensionless variables as

$$\rho_i = \frac{Tx}{2} - \frac{\eta}{2} \tag{3.15}$$

where the parameter η is defined by

$$\eta := \mu - \Phi_i + \sum_j \rho_j. \tag{3.16}$$

Since (3.15) assumes the same form as (3.10) for the bulk system, the same reasoning may be applied to allow us to conclude that in the limit $T = 0$, the only stable solutions of (3.15) are $\rho = 0$ and 1, irrespective of the value of η. Therefore, at $T = 0$ all of the sites along lines parallel with the y-axis are either empty or filled. The stable solution of the overall problem is the set $\{\rho_i^0\}$ which minimizes the functional

$$\Omega[\rho_i^0] = -\frac{\epsilon_{\rm ff}}{2} \sum_{i=1}^{\mathcal{N}} \sum_{j\neq i}^{\nu(i)} \rho_i^0 \rho_j^0 + \sum_{i=1}^{\mathcal{N}} [\Phi_i - \mu]\rho_i^0 \tag{3.17}$$

where all the ρ_i^0 are either 0 or 1. Again, this conclusion is exactly in accord with (2.6). The set of stable solutions of (3.17) or, equivalently, (2.6), constitute the 'morphologies' at $T = 0$.

4. Phase behaviour at $T = 0$

4.1. Morphologies in the limit $T = 0$

Following Pandit *et al*, we now consider the limit of vanishing temperature. This is helpful in enumerating the possible morphologies, whose number may be quite large in the case where Φ is spatially complex. Moreover, in the limit $T = 0$ the phase equilibria (i.e., the values of the chemical potential at which morphologically distinct phases coexist) can be determined analytically.

Our recipe for identification of the possible morphologies is based on a modular approach in which we construct a hierarchy of increasingly complex modules sequentially from simpler ones, starting from the bulk. Any module, which gives rise to a set of morphologies $\{\mathcal{M}\}$, consists of a juxtaposition of one or more of the previous (simpler) modules. The grand potential of a given morphology within the more complex module can be expressed as a sum of the grand potentials of the simpler ones, plus corrections which account for the breaking of bonds between nearest neighbours in the simpler modules and the making of new bonds across the interfaces between modules that make up the composite (more complex) module. The sum of all of these contributions determines the number and stability of the possible morphologies.

4.1.1. Bulk lattice gas. In the simplest case, $\Phi \equiv 0$ and all sites are equivalent. Thus, equation (2.6) reduces to

$$\Omega_{\mathrm{b}} = -\mathcal{N}(3\epsilon_{\mathrm{ff}}s_0^2 + \mu s_0) := \mathcal{N}\omega_0. \tag{4.1}$$

In equation (4.1), ω_0 is the grand-potential density of the bulk lattice gas. Because s_0 is double-valued, equation (4.1) gives two possible morphologies, namely a 'gas' characterized by $\Omega_{\mathrm{b}}^{\mathrm{g}} = 0$ corresponding to an entirely empty lattice ($s_0 = 0$) and a 'liquid' for which $\Omega_{\mathrm{b}}^{\mathrm{l}} = -\mathcal{N}(3\epsilon_{\mathrm{ff}} + \mu)$ when all sites are occupied ($s_0 = 1$). Gas and liquid phases may coexist at μ^{gl} defined through

$$\Omega_{\mathrm{b}}^{\mathrm{g}} - \Omega_{\mathrm{b}}^{l} =: \Omega_{\mathrm{b}}^{\mathrm{gl}} = 0 = \mathcal{N}(3\epsilon_{\mathrm{ff}} + \mu^{\mathrm{gl}}) \tag{4.2}$$

from which $\mu^{\mathrm{gl}}\epsilon_{\mathrm{ff}}^{-1} = -3$ is easily deduced. Thus, for $\mu < \mu^{\mathrm{gl}}$, gas is the thermodynamically stable phase, whereas for $\mu > \mu^{\mathrm{gl}}$ liquid is the stable phase.

4.1.2. Hard substrates. The next slightly more complicated situation is one in which a lattice gas is confined in the z-direction by two planar hard substrates represented by

$$\Phi_i \equiv \Phi_{\mathrm{hs}}(z_i) = \begin{cases} \infty & z_i < 1 \text{ and } z_i > n_z \\ 0 & 1 \leqslant z_i \leqslant n_z. \end{cases} \tag{4.3}$$

According to our modular approach the confined lattice gas may be viewed as a bulk system, in which $\Phi_{\mathrm{hs}}(z)$ serves to introduce 'surfaces'. We can then express the grand potential of the confined phase as

$$\Omega_{\mathrm{hs}} = \Omega_{\mathrm{b}} + \Delta\Omega \tag{4.4}$$

where Ω_{b} pertains to the bulk module and the correction $\Delta\Omega$ accounts for the interactions that are missing for molecules in the surface planes $z = 1$ and $z = n_z$. Since each nearest-neighbour interaction contributes $-\epsilon_{\mathrm{ff}}s^2/2$ to the configurational energy of the original bulk module, there are $n_x n_y$ molecules in each surface, and there are two surfaces, the total correction is $n_x n_y \epsilon_{\mathrm{ff}} s^2$. We can therefore rewrite (4.4) as

$$\Omega_{\mathrm{hs}} = n_x n_y n_z \omega_0 + n_x n_y \epsilon_{\mathrm{ff}} s_0^2 \tag{4.5}$$

where ω_0 is defined by (4.1). However, since $s_0 = 0$ or 1, no new morphologies arise. The only effect of confinement is an upward shift in the chemical potential at gas–liquid coexistence. By solving the analogue of (4.2), $\Omega^{\mathrm{g}}_{\mathrm{hs}} = \Omega^{\mathrm{l}}_{\mathrm{hs}}$, we obtain $\mu^{\mathrm{gl}}\epsilon_{\mathrm{ff}}^{-1} = -3 + 1/n_z$. As expected, this shift vanishes in the limit of large substrate separations (i.e., as $n_z \to \infty$).

4.1.3. Chemically homogeneous substrates. The situation discussed in section 4.1.2 becomes slightly more complicated if one replaces (4.3) by

$$\Phi_i \equiv \Phi_{\mathrm{hom}}(z_i) = \begin{cases} \infty & z_i < 1 \text{ and } z_i > n_z \\ -\epsilon_{\mathrm{fs}} & z_i = 1 \text{ and } z_i = n_z \\ 0 & 2 \leqslant z_i \leqslant n_z - 1 \end{cases} \tag{4.6}$$

i.e. by chemically homogeneous substrates capable of attracting the lattice gas in addition to merely confining it. It is therefore convenient to introduce an *effective* chemical potential

$$\mu_i^{\mathrm{eff}} := \mu - \Phi_i \tag{4.7}$$

to which different regions of the confined lattice gas are subject. The concept of an effective chemical potential is useful because it permits one to distinguish between the two regions (slabs) governed by $\mu_0^{\mathrm{eff}}(z_i)$ $(2 \leqslant z_i \leqslant n_z - 1)$ and $\mu_1^{\mathrm{eff}}(z_i)$ $(z_i = 1, z_i = n_z)$. The subscripts 0 and 1 on μ^{eff} now refer to all sites in the regions $\{z_i | 2 \leqslant z_i \leqslant n_z - 1\}$ and $\{z_i | z_i = 1, z_i = n_z\}$.

The possible morphologies of the lattice gas confined between homogeneous attractive substrates can thus be determined by sandwiching an $n_x \times n_y \times (n_z - 2)$ hard-substrate module (which consists of a slab of uniformly occupied ($s = 0$ or 1) sites) between two $n_x \times n_y \times 1$ hard-substrate modules (i.e., identical thin slabs of $n_x n_y$ uniformly occupied sites). Using the modular principle, we can express the grand potential of the composite 'homogeneous' module as

$$\Omega_{\mathrm{hom}} = \Omega^{[0]}_{\mathrm{hs}} + 2\Omega^{[1]}_{\mathrm{hs}} + \Delta\Omega \tag{4.8}$$

where

$$\begin{aligned} \Omega^{[0]}_{\mathrm{hs}} &:= n_x n_y[(n_z - 2)\omega_0 + \epsilon_{\mathrm{ff}} s_0^2] \\ \Omega^{[1]}_{\mathrm{hs}} &:= n_x n_y[\omega_1 + \epsilon_{\mathrm{ff}} s_1^2] \end{aligned} \tag{4.9}$$

and Ω_{hs} stands for the grand potential of the previous member of the hierarchy of modules, namely a slab between hard substrates. The index 0 denotes the central module at $\mu_0^{\mathrm{eff}} \equiv \mu$, while the index 1 pertains to the other two (identical) modules at $\mu_1^{\mathrm{eff}} = \mu + \epsilon_{\mathrm{fs}}$. Since Ω_{hs} already accounts for the breaking of bonds to create free surfaces (see the discussion in section 4.1.2), the correction $\Delta\Omega$ in (4.8) is due solely to the formation of bonds across the two interfaces and is given by $-2n_x n_y \epsilon_{\mathrm{ff}} s_0 s_1$. Therefore, we can rewrite (4.8) as

$$\Omega_{\mathrm{hom}} = n_x n_y \psi \tag{4.10}$$

where

$$\psi := 2(\omega_1 + \epsilon_{\mathrm{ff}} s_1^2) + (n_z - 2)\omega_0 + \epsilon_{\mathrm{ff}} s_0^2 - 2\epsilon_{\mathrm{ff}} s_0 s_1. \tag{4.11}$$

Since s_0 and s_1 can assume values 0 or 1 independently, four different morphologies arise from the homogeneous module. These can be identified by sets of occupation numbers $\mathcal{M} = \{s_0, s_1\}$, where $s_0 = 0$ or 1 and $s_1 = 0$ or 1 are the uniform occupation numbers over the central and outer slabs, respectively. For example, $\mathcal{M}^{\mathrm{g}} = \{0, 0\}$ corresponds to gas, and $\mathcal{M}^{\mathrm{m}} = \{0, 1\}$ to a monolayer film on each substrate. The grand potentials Ω^α associated with the possible morphologies $\mathcal{M}^\alpha$ can be determined from (4.10) in closed form, where Ω^α is a linear function of μ. Thus, the values of the chemical potential at which morphologies (say α and β) can

coexist are determined by the intersection between Ω^α and Ω^β, that is where $\Omega^\alpha = \Omega^\beta$. (Note that the intersection must lie below all other curves Ω^γ for other morphologies.) The locations, as well as the total number of intersections, depend on the parameters of the model (i.e., n_z, $\epsilon_{\rm fs}/\epsilon_{\rm ff}$, etc). In section 5.2.2 we see that the monolayer film can indeed become the stable phase when $\epsilon_{\rm fs}/\epsilon_{\rm ff} = 1.5$.

4.1.4. Chemically heterogeneous substrates. Consider now the prototype: a lattice gas between substrates decorated with strongly attractive stripes (well depth $\epsilon_{\rm fs}$) that alternate periodically with weakly attractive stripes (well depth $\epsilon_{\rm fw}$) in the x-direction. Within one period the potential can be represented as

$$\Phi_i \equiv \Phi_{\rm het}(x_i, z_i) = \begin{cases} \infty & z_i < 1 \text{ and } z_i > n_z \\ \begin{cases} -\epsilon_{\rm fs} & 1 \leqslant x_i \leqslant n_{\rm s} \\ -\epsilon_{\rm fw} & n_{\rm s} < x_i \leqslant n_x \end{cases} & z_i = 1 \text{ and } z_i = n_z \\ 0 & 2 \leqslant z_i \leqslant n_z - 1. \end{cases} \tag{4.12}$$

Again following the modular principle, we can enumerate the possible morphologies by juxtaposing (in the x-direction) two modules corresponding to the previous, simpler one: the lattice gas between homogeneous attractive substrates. Thus, we can write the grand potential as

$$\Omega_{\rm het} = \Omega^{[\rm w]}_{\rm hom} + \Omega^{[\rm s]}_{\rm hom} + \Delta\Omega \tag{4.13}$$

where from (4.10)

$$\Omega^{[\rm u]}_{\rm hom} = n_{\rm u} n_y \psi_{\rm u} \qquad {\rm u} = {\rm s}, {\rm w} \tag{4.14}$$

and from (4.11)

$$\psi_{\rm u} = 2(\omega^{\rm u}_1 + \epsilon_{\rm ff} s^{\rm u}_1 s^{\rm u}_1) + (n_z - 2)\omega^{\rm u}_0 + \epsilon_{\rm ff} s^{\rm u}_0 s^{\rm u}_0 - 2\epsilon_{\rm ff} s^{\rm u}_0 s^{\rm u}_1 \qquad {\rm u} = {\rm s}, {\rm w}. \tag{4.15}$$

$\Omega^{[\rm s]}_{\rm hom}$ and $\Omega^{[\rm w]}_{\rm hom}$ are the grand potentials of the lattice gas between strongly attractive substrates of width $n_{\rm s}$ and between weakly attractive substrates of width $n_{\rm w} = n_x - n_{\rm s}$. Note that the regions of the composite module now carry two indices, one denoting the strength of the attraction (w or s) and the other denoting the particular slab of the 'homogeneous' module (0 referring to the central slab and 1 to the outer slabs).

The correction in (4.13) can be derived as follows. We must first create surfaces by breaking bonds between nearest neighbours across a plane (parallel with the y–z plane) in the 'homogeneous' module. This process increases U (and hence Ω) by the amounts $n_y\epsilon_{\rm ff}[2s^{\rm u}_1 s^{\rm u}_1 + (n_z - 2)s^{\rm u}_0 s^{\rm u}_0]$ for weak (u = w) and strong (u = s) substrates. We must then join the strong and weak 'homogeneous' modules by forming bonds across the interfaces. This joining decreases U by $n_y\epsilon_{\rm ff}[2s^{\rm w}_1 s^{\rm s}_1 + (n_z - 2)s^{\rm w}_0 s^{\rm s}_0]$. Thus, the total grand potential for the 'heterogeneous' module can be expressed as

$$\Omega_{\rm het} = n_y[n_{\rm s}\psi_{\rm s} + n_{\rm w}\psi_{\rm w} + \chi_{\rm ss} + \chi_{\rm ww} - 2\chi_{\rm sw}] \tag{4.16}$$

where

$$\begin{aligned} \chi_{\rm uu} &= \epsilon_{\rm ff}[2s^{\rm u}_1 s^{\rm u}_1 + (n_z - 2)s^{\rm u}_0 s^{\rm u}_0] \qquad {\rm u} = {\rm s}, {\rm w} \\ \chi_{\rm sw} &= \epsilon_{\rm ff}[2s^{\rm w}_1 s^{\rm s}_1 + (n_z - 2)s^{\rm w}_0 s^{\rm s}_0]. \end{aligned} \tag{4.17}$$

A consequence of the lower symmetry of the prototype is a larger number of possible morphologies. Inspection of (4.15)–(4.17) reveals that the grand potential is determined by the set $\mathcal{M} := \{s^{\rm w}_0, s^{\rm s}_0, s^{\rm w}_1, s^{\rm s}_1\}$, where each occupation number can independently assume the value 0 or 1. Thus, 16 different morphologies are possible *in principle*. This fairly large

number can be reduced substantially on physical grounds (i.e. by taking into account the relative magnitudes of $\epsilon_{\rm fs}$, $\epsilon_{\rm fw}$, and $\epsilon_{\rm ff}$). For example, if both $\epsilon_{\rm fs}$ and $\epsilon_{\rm fw}$ are small compared to $\epsilon_{\rm ff}$, the morphology characterized by $\mathcal{M} = \{0, 0, 1, 1\}$ is physically not sensible because it refers to a situation where sites at which the lattice gas is exposed to a reduced total attraction (i.e., in the immediate vicinity of the substrate) are occupied whereas energetically more favourable $(n_z - 2)$ bulk sites remain empty. By similar considerations most of the remaining morphologies can be ruled out, without the necessity of calculating their grand potentials.

4.2. Thermodynamically stable morphologies at $T = 0$

The analysis of potentially possible morphologies of the prototype in section 4.1.4 can now be employed to construct the phase diagram at $T = 0$. Henceforth we employ the dimensionless units defined in section 3.2

As an example we consider the case $n_{\rm s} = n_{\rm w} = 10$ ($n_x = 20$), $n_z = 10$, $\epsilon_{\rm fw} = 0.0$, and $0.0 \leqslant \epsilon_{\rm fs} \leqslant 2.0$. With the aid of figure 1 it can be seen that the only physically sensible morphologies are characterized by $\mathcal{M}^{\rm g} = \{0, 0, 0, 0\}$ (empty lattice, i.e. 'gas'), $\mathcal{M}^{\rm l} = \{1, 1, 1, 1\}$ (full lattice, i.e. 'liquid'), $\mathcal{M}^{\rm d} = \{0, 0, 0, 1\}$ (liquid-filled lanes stabilized by strongly adsorbing stripe, i.e. 'droplets'), $\mathcal{M}^{\rm b} = \{0, 1, 0, 1\}$ (a fluid 'bridge' connecting strongly adsorbing stripes), and $\mathcal{M}^{\rm v} = \{1, 1, 0, 1\}$ (gas-filled lanes immersed in high-density fluid, i.e. 'vesicles'). Explicit expressions for the grand potentials for these morphologies are derived in appendix A.

Thermodynamic consistency requires the inequality

$$\left(\frac{\partial\,\Omega}{\partial\mu}\right)_T = -N \leqslant 0 \tag{4.18}$$

to hold for any morphology, where $N < \mathcal{N}$ is the number of occupied sites. For $T = 0$, N is independent of μ. In other words, because each morphology is in its ground state, there are no density fluctuations. That is,

$$\left(\frac{\partial^2\Omega}{\partial\mu^2}\right)_{T=0} = 0 \tag{4.19}$$

so the curve $\Omega(\mu)$ is a straight line with negative slope for each morphology (see figure 2(a)). The curves plotted in figure 2(a) indicate that the higher the average density of the lattice gas is, the larger is the magnitude of the slope of $\Omega(\mu)$, as one would expect from (4.18).

On account of the different slopes of $\Omega(\mu)$ for the various morphologies considered in figure 2, one expects intersections $\mu^{\alpha\beta}$ between $\alpha\beta$-pairs of grand-potential curves defined via

$$\Omega^{\alpha}(\mu_x^{\alpha\beta}) = \Omega^{\beta}(\mu_x^{\alpha\beta}). \tag{4.20}$$

We can solve (4.20) analytically for $\mu_x^{\alpha\beta}$ using the explicit expressions for $\Omega^{\alpha}(\mu)$ given in appendix A, although for the sake of conciseness we refrain from displaying the solutions. However, it seems worthwhile noting that for $\epsilon_{\rm fw} = 0$, $\mu_x^{{\rm g}\beta}$ depends linearly on $\epsilon_{\rm fs}$ regardless of β. That is, with increasing $\epsilon_{\rm fs}$, $\mu_x^{{\rm g}\beta}$ is shifted to more negative values. At the same time, $\mu_x^{\alpha\beta}$ ($\alpha, \beta \neq {\rm g}$) is independent of $\epsilon_{\rm fs}$. Thus, if for a given substrate geometry (i.e., n_x, n_z, $n_{\rm s}$) $\mu_x^{\alpha\beta}$ refers to coexistence between metastable (non-gas) morphologies, these can never become stable at $T = 0$, no matter how great the attraction of the 'strong' stripe becomes.

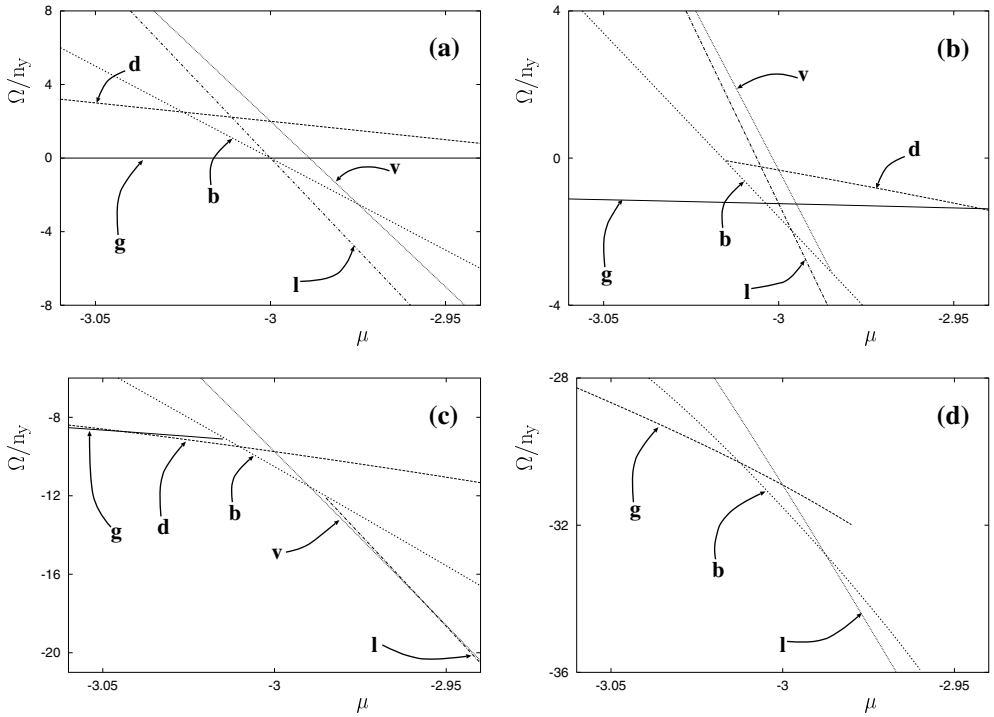

Figure 2. The grand potential $\Omega^{\alpha}(\mu)/n_y$ versus chemical potential μ for various morphologies $\alpha =$ g (gas), d (droplet), b (bridge), v (vesicle), and l (liquid) indicated in the figure. In all cases, $\epsilon_{\rm fs} = 1.0$, $\epsilon_{\rm fw} = 0.0$. (a) $T = 0$, (b) $T = 0.6$, (c) $T = 0.9$, (d) $T = 1.2$.

5. Phase behaviour for $T > 0$

5.1. Grand-potential curves for $T > 0$

For $T > 0$ analytic determination of the phase diagram is no longer possible. Instead we solve (3.8) numerically by the iterative procedure detailed in [17], using the morphologies at $T = 0$ as starting solutions. Once the set $\boldsymbol{\rho} := \{\rho_1, \rho_2, \ldots, \rho_{\mathcal{N}}\}$ has been determined the grand potential can be obtained from (3.6).

To investigate the effects of varying T we consider the case $\epsilon_{\rm fw} = 0.0$ and $\epsilon_{\rm fs} = 1.0$, where the interaction of a molecule with the 'weak' stripe is purely repulsive (i.e., hard substrate) and the interaction with the 'strong' stripe is characterized by $\epsilon_{\rm fs} \equiv \epsilon_{\rm ff}$. Thus, for molecules located at sites in the planes $z = 1$ and $z = n_z$, the interaction with the 'strong' stripes exactly compensates for the interaction with the nearest neighbour that has been lost on account of the creation of the 'surfaces' of the hard-substrate module. Figure 2(a) shows that for $T = 0$ a triple point $\mu_{\rm tr}^{\rm gbl} = -3.000$ exists at which gas, liquid, and bridge phases coexist. Following the evolution of $\Omega^{\alpha}(\mu)$ for physically sensible morphologies, one notices from the plot in figure 2(b) that for $T = 0.6$ the triple point has given way to a narrow one-phase region $-3.004 < \mu < -2.998$ in which bridge phases are thermodynamically stable. Hence, for $\{(T, \mu)|T = 0.6, \mu < -3.004\}$ the gas phases are thermodynamically stable whereas this is the case for the liquid phases over the range $\{(T, \mu)|T = 0.6, \mu > -2.998\}$.

This picture changes substantially for $T = 0.9$ (figure 2(c)). Now the gas phases are stable for thermodynamic states $\{(T, \mu)|T = 0.9, \mu < -3.044\}$. Over the range

$\{(T,\mu)|T = 0.9, -3.044 < \mu < -3.010\}$ the droplet morphology ($\mathcal{M}^{\mathrm{d}} = \{0,0,0,1\}$ for $T = 0$) represents the thermodynamically stable phase. At $\mu_x^{\mathrm{gd}} = -3.044$ gas and droplet phases coexist. The region of bridge phases, $\{(T,\mu)|T = 0.9, -3.010 < \mu < -2.990\}$, has considerably widened compared with $T = 0.6$ (figure 2(b)). Bridge and droplet phases coexist at $\mu_x^{\mathrm{db}} = -3.010$ whereas bridge and vesicle phases ($\mathcal{M}^{\mathrm{v}} = \{1,1,0,1\}$ for $T = 0$) coexist at $\mu_x^{\mathrm{bv}} = -2.990$. Vesicle phases are thermodynamically stable over the range $\{(T,\mu)|T = 0.9, -2.990 < \mu < -2.956\}$, eventually coexisting with liquid at $\mu_x^{\mathrm{vl}} = -2.956$, which is then stable for all larger chemical potentials.

For an even higher temperature $T = 1.2$ one deduces from figure 2(d) that only gas, bridge, and liquid phases are thermodynamically stable over the respective ranges $\{(T,\mu)|T = 1.2, \mu < -3.013\}$, $\{(T,\mu)|T = 1.2, -3.013 < \mu < -2.988\}$, and $\{(T,\mu)|T = 1.2, \mu > -2.988\}$ where $\mu_x^{\mathrm{gb}} = -3.013$ and $\mu_x^{\mathrm{bl}} = -2.988$. One also realizes from figure 2(d) that $(\partial^2\Omega/\partial\mu^2)_T < 0$ corresponding to a non-vanishing isothermal compressibility $\kappa_T > 0$ for all three phases. At μ_x^{gb} and μ_x^{bl}, κ_T changes discontinuously but remains finite as expected.

5.2. Phase diagrams

5.2.1. The case $\epsilon_{fw} = 0.0$, $\epsilon_{fs} > 0.0$. From the consideration of grand-potential curves in section 3.1 we are now in a position to determine lines of discontinuous phase transitions (i.e., coexistence lines) through the analogue of (4.20)

$$\Omega^{\alpha}[\mu_x^{\alpha\beta}(T)] = \Omega^{\beta}[\mu_x^{\alpha\beta}(T)] \tag{5.1}$$

where $\mu_x^{\alpha\beta}(T)$ stands for the coexistence line, that is the set of values of the chemical potential at which morphologies α and β coexist at temperature T. The phase diagram can then be represented by

$$\mu_x(T) = \bigcup_{\alpha,\beta} \mu_x^{\alpha\beta}(T) \qquad \forall \alpha \neq \beta \tag{5.2}$$

i.e. the union of all coexistence lines between all pairs of morphologies. Thus, one can perceive $\mu_x(T)$ as a 'web' of coexistence lines, whose structure depends implicitly on system parameters ϵ_{fw}, ϵ_{fs}, n_{w}, n_{s}, and n_z. As these parameters vary, the web evolves. Figure 3 illustrates the impact of increasing attraction between the lattice gas and the 'strong' stripe. For $\epsilon_{\mathrm{fs}} = 0.5$ figure 3(a) reveals a tiny one-phase region for bridge phases indicated by the bifurcation in $\mu_x(T)$ at $T \simeq 1.375$. The coexistence lines involving bridge phases terminate at the respective critical temperatures $T_{\mathrm{c}}^{\mathrm{gb}} \simeq 1.461$ and $T_{\mathrm{c}}^{\mathrm{bl}} \simeq 1.440$. One also notes a bifurcation in $\mu_x(T)$ at $T \simeq 0.980$, indicating the existence of a vesicle phase. The vesicle–liquid coexistence line ends at its critical temperature $T_{\mathrm{c}}^{\mathrm{vl}} \simeq 1.005$.

Increasing the fluid–substrate interaction to $\epsilon_{\mathrm{fs}} = 1.0$ (figure 3(b)) causes $\mu_x(T)$ to move down to lower chemical potentials compared with the plot in figure 3(a). The gas–bridge–liquid triple point has also shifted all the way to $T = 0$ (see also figure 2(a)), so the one-phase region of bridge phases is now much wider compared with the case $\epsilon_{\mathrm{fs}} = 0.5$. At the same time $T_{\mathrm{c}}^{\mathrm{vl}}$ has not changed at all but the coexistence line $\mu_x^{\mathrm{vl}}(T)$ is longer now. However, a new bifurcation appears at $T = \simeq 0.815$, which corresponds to the appearance of a droplet phase that can coexist with gas or bridge phases. We note that the phase diagram appears to be precisely symmetric about the line $\mu_{\mathrm{c}} = -3$.

For even larger $\epsilon_{\mathrm{fs}} = 1.1$ one sees from figure 3(c) that the gas–bridge–liquid triple point vanishes; that is, even for $T = 0$ a range of chemical potentials exists over which bridges are the thermodynamically stable phases. This effect results from a lowering of the temperature at

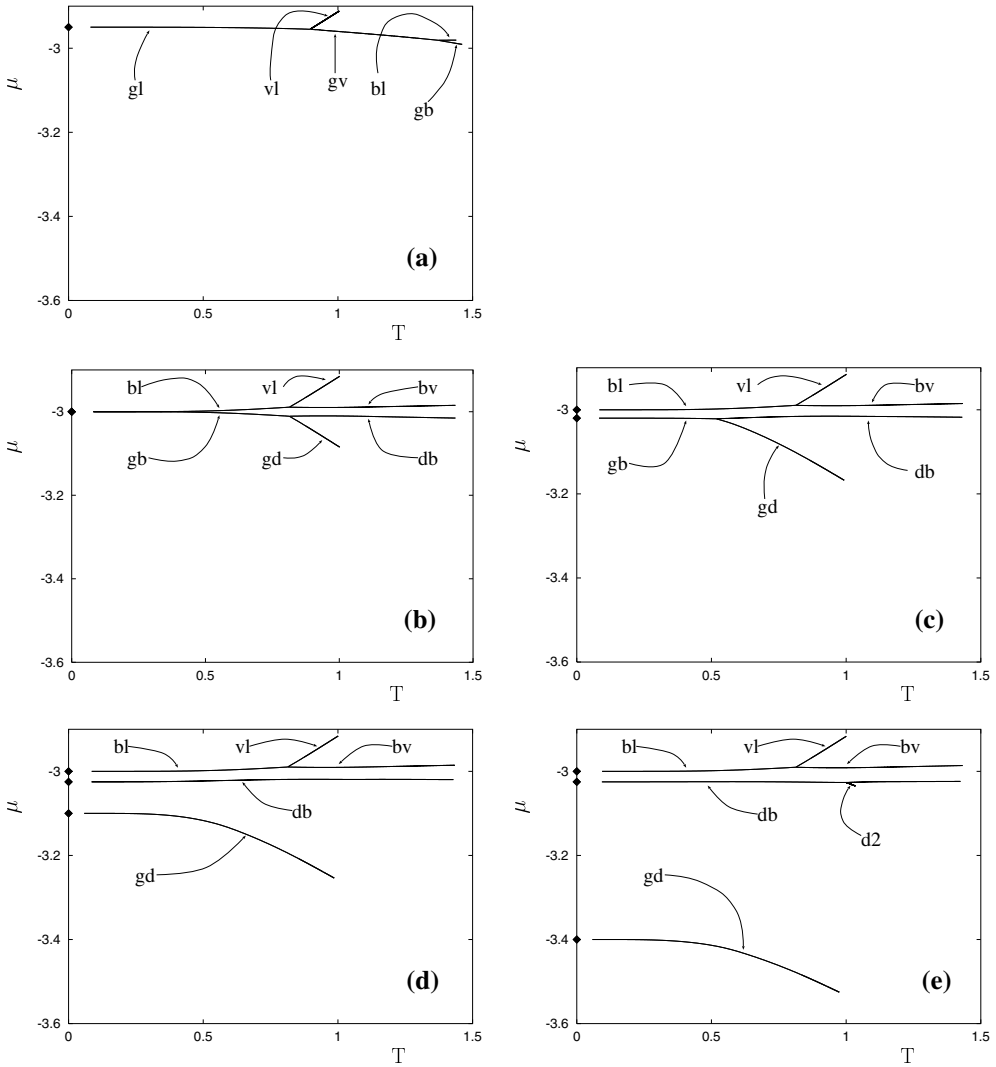

Figure 3. Phase diagrams in the μ–T representation for $\epsilon_{\rm fw} = 0$. (a) $\epsilon_{\rm fs} = 0.5$, (b) $\epsilon_{\rm fs} = 1.0$, (c) $\epsilon_{\rm fs} = 1.1$, (d) $\epsilon_{\rm fs} = 1.2$, (e) $\epsilon_{\rm fs} = 1.5$. ♦: analytical solution for $T = 0$.

which the 'droplet' bifurcation occurs, along with a shift of $\mu_x^{\rm gb}(T)$ and $\mu_x^{\rm gd}(T)$ toward lower values of μ for $T < T_{\rm c}^{\rm gd}$. As before, however, all four critical temperatures remain unaltered.

A slight further increase of the strength fluid–substrate attraction to $\epsilon_{\rm fs} = 1.2$ eventually causes $\mu_x^{\rm gd}(T)$ to become detached from the other coexistence lines as the plot in figure 3(d) clearly shows. The remainder of the phase diagram appears to be unaffected by the increase of $\epsilon_{\rm fs}$. Consequently, one finds three chemical potentials for $T = 0$ at which pairs of phases (i.e., gas–droplet, droplet–bridge, bridge–liquid) coexist. The one-phase region of droplet phases is already quite large. It increases further if the interaction of the lattice gas with the 'strong' stripe is increased to $\epsilon_{\rm fs} = 1.5$ (see figure 3(e)). For this value of $\epsilon_{\rm fs}$ one notices the appearance of a very short additional coexistence line beginning at $T_{\rm tr}^{\rm bd2} \simeq 1.001$ and $\mu \simeq -3.027$ with negative slope. An inspection of the local densities indicates that this coexistence line reflects

layering transitions between droplet phases and new bilayer droplet phases (2) localized at the 'strong' stripe. The layering transitions disappear at a critical temperature $T_c^{d2} \simeq 1.035$.

5.2.2. The case $\epsilon_{fs} > 0$, $\epsilon_{fw} > 0$. Plots in figure 4 illustrate variations of $\mu_x(T)$ with increasing interaction between lattice gas and the 'weak' stripe. Comparing figure 4(a) with figure 4(b) one notices that $\mu_x^{gd}(T)$ starting at $\mu = -3.400$ for $T = 0$ remains unaffected. However, the vesicle and layered phases, both visible in figure 4(a), disappear. At the same time the triple-point temperature corresponding to droplet–bridge–liquid coexistence is significantly raised to $T_{tr}^{dbl} \simeq 1.310$.

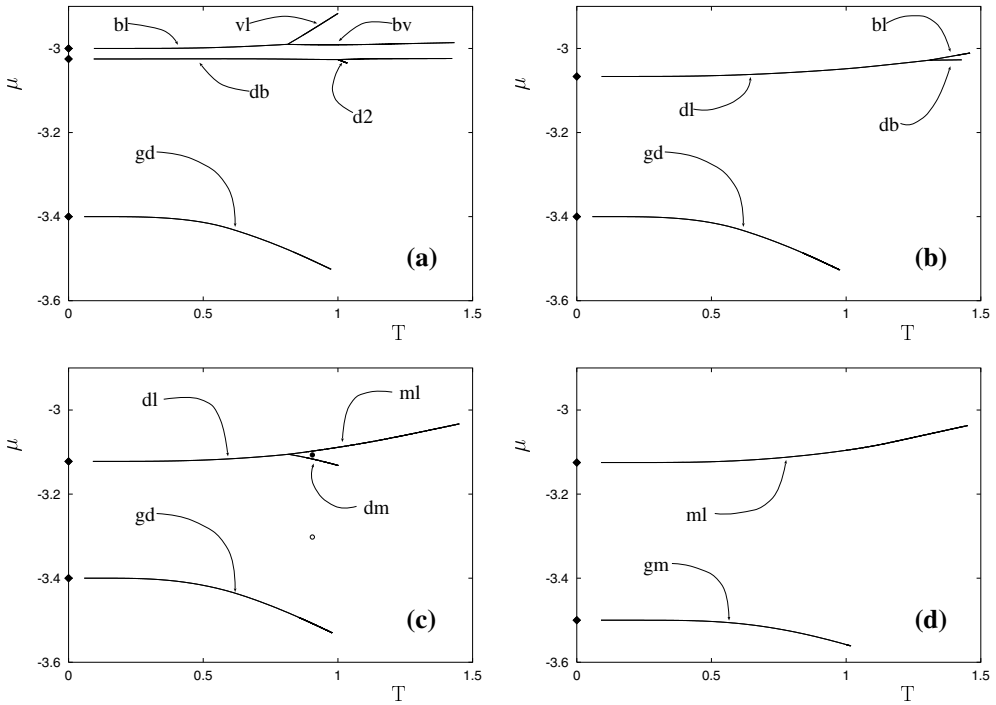

Figure 4. As figure 3, but for $\epsilon_{fs} = 1.5$. (a) $\epsilon_{fw} = 0.0$, (b) $\epsilon_{fw} = 0.5$, (c) $\epsilon_{fw} = 1.0$, (d) $\epsilon_{fw} = 1.5$. Open and filled circles in figure 4(c) signify thermodynamic states for which local densities are plotted in figure 6(a) and figure 6(b), respectively. ♦: analytical solution for $T = 0$.

As ϵ_{fw} increases further to 1.0, plots in figure 4(c) show that $\mu_x^{gd}(T)$ is still unaffected. On the other hand, the bifurcation appearing in figure 4(b) apparently shifts to a temperature of about 0.817. However, an inspection of the phase diagrams in the equivalent T–ρ representation in figure 5(a) and figure 5(b) shows that the bifurcation temperature is actually not associated with bridge phases, which have already become metastable for this ϵ_{fw} (see figure 5(b)). Instead the coexistence line branching off at $T_{tr}^{dml} \simeq 0.817$ corresponds to a line of discontinuous transitions between droplet phases and a monolayer (m) phases adsorbed on the *entire* substrate (see figure 6(a), figure 6(b)) and may thus be regarded as a different type of layering transition triggered predominantly by the 'weak' part of the substrate.

If $\epsilon_{fw} = 1.5$ the decorated substrate degenerates to a chemically homogeneous one wetted by the lattice gas. In this case $\mu_x(T)$ consists of $\mu_x^{gm}(T)$ ending at $T_c^{gm} \simeq 1.018$ and $\mu_x^{ml}(T)$ terminating at its critical temperature $T_c^{ml} \simeq 1.452 < T_c^{bulk} = \frac{3}{2}$ on account of confinement

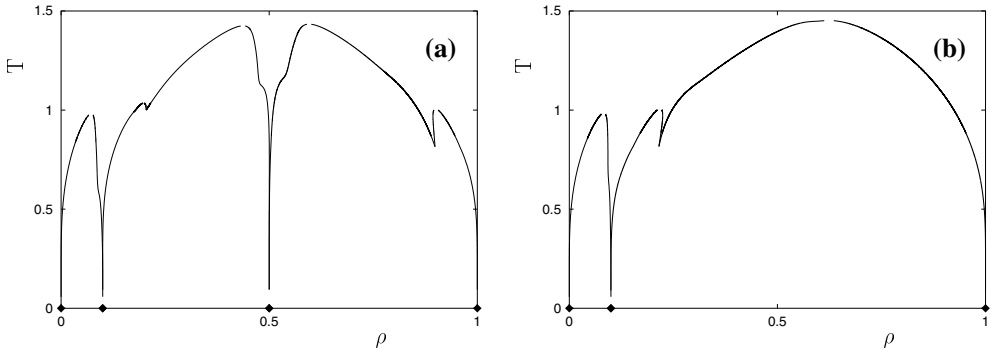

Figure 5. Phase diagrams in the T–ρ representation for $\epsilon_{\rm fs} = 1.5$. (a) $\epsilon_{\rm fw} = 0.0$, (b) $\epsilon_{\rm fw} = 1.0$ corresponding to figure 4(a) and figure 4(c), respectively. ♦: analytical solution for $T = 0$. Note that in the immediate vicinity of the critical points the phase diagram could not be determined because of the failure of the numerical method to converge (see [17]).

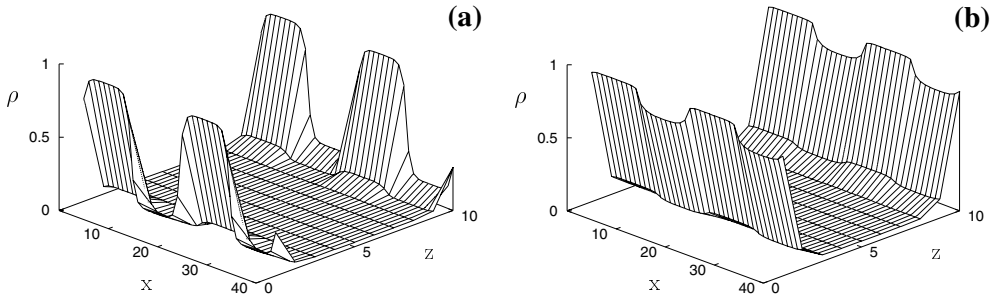

Figure 6. The local density $\rho(x, z)$ of lattice gases between prototypal chemically decorated substrates (see figure 1) where $\epsilon_{\rm fw} = 1.0$, $\epsilon_{\rm fs} = 1.5$, and $T = 0.9$ (see figure 4(c)). (a) $\mu = -3.30$, (b) $\mu = -3.11$.

where we use superscript 'm' to indicate that the droplet phase has been replaced by the monolayer as indicated by the representative plot of the local density in figure 6(b). However, in the present case the local density in this monolayer no longer depends on x.

6. Summary and conclusions

This work is concerned with the phase behaviour of a prototype for fluids confined by chemically heterogeneous substrates: a simple fluid (composed of structureless molecules) constrained between two identical planar substrates that consist of weakly attractive stripes alternating periodically with strongly attractive stripes in one transverse direction. The fluid is treated as a lattice gas, the positions of molecules being constrained to sites of a simple cubic lattice. At most a single molecule can occupy a given site. Only nearest-neighbour interactions (attractions) are taken into account and these are described by square-well potentials: $\epsilon_{\rm ff}$ is the well depth of the fluid–fluid attraction; $\epsilon_{\rm fw}$ and $\epsilon_{\rm fs}$ are the well depths of the attraction of a fluid molecule for the strong and weak stripes, respectively. The model is characterized by the well depths as well as by the dimensions of weak and strong stripes, $n_{\rm w}$ and $n_{\rm s}$, the distance between the substrates n_z, the chemical potential μ, and the absolute temperature T.

We obtain an explicit expression for the *exact* grand potential at $T = 0$ in terms of model parameters and the occupation numbers of the lattice sites s_i, which can be 0 or 1. We use

this expression to determine the possible structural types of phase (morphologies) that can exist (or coexist) at $T = 0$. Utilizing Bogoliubov's variational principle, we derive mean-field equations for the (ensemble) average occupation numbers $\boldsymbol{\rho} = \{\rho_1, \rho_2, \ldots, \rho_{\mathcal{N}}\}$ for $T > 0$. Using the morphologies at $T = 0$ as starting trial solutions, we solve the Euler–Lagrange equations iteratively for $\boldsymbol{\rho}$, from which we obtain the corresponding grand potentials. In turn we use the grand potentials as functions of μ and T to deduce the phase diagram for the prototype. We also demonstrate that the mean-field solution becomes exact in the limit of vanishing temperature.

To enumerate the possible morphologies at $T = 0$, we construct a hierarchy of modules (each module yields a *set* of morphologies) of increasing complexity, starting with the simplest module, namely that for the bulk, which yields the simplest morphologies—'gas' or 'liquid'. At any given level of the hierarchy the module is constructed by juxtaposing the simpler modules of the previous level. Thus, the grand potential associated with the more complex (composite) module is expressible as a sum of the grand potentials of the simpler modules, plus a correction that accounts for the breaking of bonds (interactions) in the simpler modules and the making of new bonds at the interfaces between these modules making up the composite. Explicit analytic expressions for the grand potentials for the possible morphologies at $T = 0$ can be obtained in this way and used to determine which morphologies are stable over which ranges of μ and consequently which morphologies can coexist.

For the prototype we find 16 possible morphologies, which are specified by sets of occupation numbers $\mathcal{M} = \{s_0^{\mathrm{w}}, s_0^{\mathrm{s}}, s_1^{\mathrm{w}}, s_1^{\mathrm{s}}\}$, where the indices on s identify the region (slab) of the system. However, depending on the parameters, only a limited subset can exist at $T = 0$. The μ–T representation of the phase diagram at $T = 0$ consists of a set of points along the ordinate. As T increases from 0, the mean-field solutions yield a μ–T phase diagram ($\mu_x(T)$) that 'grows' from these points. We explored two principal cases:

(a) $\epsilon_{\mathrm{fw}} = 0.0$, for which, in addition to the gas, bridge, and liquid morphologies, droplet and vesicle morphologies also arise;
(b) $\epsilon_{\mathrm{fw}} > 0.0$, for which new 'layered' morphologies may appear, which involve more than just a monolayer, despite the short-range nature of the fluid–substrate attraction.

This richness of the phase behaviour was missed altogether in all previous work employing this [13–17] or closely related models [11,12] of fluids confined between chemically decorated substrates.

For the hierarchy of modules considered here (see section 4.1), namely bulk, hard-substrate, homogeneous, and heterogeneous, the number of possible morphologies enumerated are 2, 2, 4, and 16, respectively. The number of stable morphologies, and consequently the complexity of the phase diagram, seem to increase rapidly with the geometrical complexity of the decoration of the substrates. An increase in complexity of the decoration is also accompanied by a decrease in the symmetry of Φ. The extreme situation might be a fluid in a 'random' porous medium, where Φ lacks symmetry entirely. The modular approach to delineation of 'morphologies', which is based on the symmetry inherent in the modules, would obviously be to no avail in the case of the random porous medium. Indeed, the possible morphologies would seem to be as numerous as the ways of arranging 0s and 1s on the $\mathcal{N}$ lattice sites, namely $2^{\mathcal{N}}$. This would yield $2^{\mathcal{N}}$ densely bunched grand-potential curves ($\gtrsim 10^{30}$ for the case $\mathcal{N} = 200$, as used for the calculations reported here), which would be impossible to sort out in order to determine the 'phase diagram' at $T = 0$, let alone the complete phase diagram. The use of morphologies as a basis for exploring the phase behaviour of this extreme system breaks down. This is in accord with recent work by Tarjus *et al*, who consider sorption isotherms in a random porous medium [27]. On the basis of a local mean-field approach

similar to the one that we use here, they show that the true equilibrium states along the sorption isotherm lie within an envelope of a large (if not infinite) number of metastable states.

The present study also has important implications for the determination of $\mu_x(T)$ by alternative techniques where the grand potential is not known as a functional of the local density. For example, one can use Monte Carlo methods to obtain $\mu_x(T)$ via thermodynamic integration [28, 29]. Thermodynamic integration generally proceeds by starting from states at $T = 0$, $T = \infty$ or $\mu = \pm\infty$ where Ω can be estimated reliably [28, 29]. To obtain Ω for the state of interest at some T and μ, one may determine Ω along a suitable path in thermodynamic state space connecting initial and final states. This approach is based upon the implicit assumption that the path does not cross a line of discontinuous phase transitions. Finding such a path becomes crucial and non-trivial in more complex systems, as the present work shows.

Acknowledgments

We are grateful to Professor R Evans for helpful comments on the original manuscript. We acknowledge financial support from the Sonderforschungsbereich 448 'Mesoskopisch strukturierte Verbundsysteme'. DJD is especially grateful for the generous hospitality of the Iwan-N-Stranski-Institut für Physikalische und Theoretische Chemie.

Appendix A. Grand potentials for various morphologies at $T = 0$

Using (4.15), (4.16), and (4.17), we derive expressions for the grand potential of various morphologies (designated by $\mathcal{M} = \{s_0^{\mathrm{w}}, s_0^{\mathrm{s}}, s_1^{\mathrm{w}}, s_1^{\mathrm{s}}\}$) of the lattice gas confined between chemically striped substrates in the limit $T = 0$. The trivial one of these is the 'gas', that is the empty lattice $\mathcal{M}^{\mathrm{g}} = (0, 0, 0, 0)$, for which

$$\Omega^{\mathrm{g}}(\mu) \equiv 0. \tag{A.1}$$

The simplest non-trivial morphology is the 'droplet' $\mathcal{M}^{\mathrm{d}} = (0, 0, 0, 1)$. Its grand potential is given by

$$\Omega^{\mathrm{d}}(\mu) = n_y\left[-2n_{\mathrm{s}}\left(\frac{\nu-2}{2}+\mu\right)+2-2n_{\mathrm{s}}\epsilon_{\mathrm{fs}}\right] \tag{A.2}$$

where ν (=6) is the number of nearest neighbours. Eventually, a 'bridge' morphology ($\mathcal{M}^{\mathrm{b}} = \{1, 0, 1, 0\}$) characterized by

$$\Omega^{\mathrm{b}}(\mu) = n_y\left[-n_{\mathrm{s}}n_z\left(\frac{\nu}{2}+\mu\right)+n_z+n_{\mathrm{s}}-2n_{\mathrm{s}}\epsilon_{\mathrm{fs}}\right] \tag{A.3}$$

may form connecting the strongly attractive stripes of the substrates along the z-direction. It is also conceivable that under favourable conditions a 'vesicle' ($\mathcal{M}^{\mathrm{v}} = \{1, 1, 1, 0\}$) may exist. Its grand potential is given by

$$\Omega^{\mathrm{v}}(\mu) = n_y\left[(2n_{\mathrm{w}}-n_xn_z)\left(\frac{\nu}{2}+\mu\right)+2+n_x-2n_{\mathrm{s}}\epsilon_{\mathrm{fs}}\right]. \tag{A.4}$$

Eventually, all lattice sites may be occupied to yield a morphology to which we refer as 'liquid' ($\mathcal{M}^{\mathrm{l}}(1, 1, 1, 1)$). The grand potential of this liquid is given by

$$\Omega^{\mathrm{l}}(\mu) = n_y\left[-n_xn_z\left(\frac{\nu}{2}+\mu\right)+n_x-2n_{\mathrm{s}}\epsilon_{\mathrm{fs}}-2n_{\mathrm{w}}\epsilon_{\mathrm{fw}}\right]. \tag{A.5}$$

The morphology having the smallest grand potential at a given value of μ is the thermodynamically stable phase at $T = 0$. If $\Omega^{\alpha}(\mu^{\alpha\beta}) = \Omega^{\beta}(\mu^{\alpha\beta})$ at a particular value of $\mu^{\alpha\beta}$, the

morphologies α and β coexist, provided that the common value of the grand potential is less than Ω^{γ} for any other morphology $\mathcal{M}^{\gamma}$. Using the formulae for Ω^{α} given in (A.1)–(A.5), we can obtain closed expressions for the coexistence points $\mu^{\alpha\beta}$ as functions of the parameters of the model.

References

[1] Tolfree D W L 1998 *Rep. Prog. Phys.* **61** 313
[2] Burmeister F, Schläfle C, Keilhofer B, Bechinger C, Boneberg J and Leiderer P 1998 *Adv. Mater.* **10** 495
[3] Bönsch P, Wüllner D, Schrimpf T, Schlachletzki A and Lacmann R 1998 *J. Electrochem. Soc.* **145** 1273
[4] Kumar A and Whitesides G M 1993 *Appl. Phys. Lett.* **63** 2002
[5] Drelich J, Miller J D, Kumar A and Whitesides G M 1994 *Colloids Surf.* A **93** 1
[6] Wilbur J L, Kumar A, Kim E and Whitesides G M 1994 *Adv. Mater.* **6** 600
[7] Knight J B, Vishwanath A, Brody J P and Austin R H 1998 *Phys. Rev. Lett.* **80** 3863
[8] Grunze M 1999 *Science* **283** 41
[9] Casagrande C, Fabre P, Raphaël E and Veyssié M 1989 *Europhys. Lett.* **9** 251
[10] de Gennes P G 1991 *Rev. Mod. Phys.* **64** 645
[11] Röcken P and Tarazona P 1996 *J. Chem. Phys.* **105** 2034
[12] Röcken P, Somoza A, Tarazona P and Findenegg G H 1998 *J. Chem. Phys.* **108** 8689
[13] Schoen M and Diestler D J 1997 *Chem. Phys. Lett.* **270** 339
[14] Schoen M and Diestler D J 1997 *Phys. Rev.* E **56** 4427
[15] Bock H and Schoen M 1999 *Phys. Rev.* E **59** 4122
[16] Bock H and Schoen M 2000 *J. Phys.: Condens. Matter* **12** 1545
[17] Bock H and Schoen M 2000 *J. Phys.: Condens. Matter* **12** 1569
[18] Gau H, Herminghaus S, Lenz P and Lipowsky R 1999 *Science* **283** 46
[19] Lipowsky R, Lenz P and Swain P S 1999 *Colloids Surf.* A **161** 3
[20] Pandit R, Schick M and Wortis M 1982 *Phys. Rev.* B **26** 5112
[21] de Oliveira M J and Griffiths R B 1978 *Surf. Sci.* **71** 687
[22] Bruno E, Marini Bettolo Marconi U and Evans R 1987 *Physica* A **141** 187
[23] Ebner C 1980 *Phys. Rev. A* **22** 2776
[24] Callen H B 1985 *Thermodynamics and an Introduction to Thermostatics* 2nd edn (New York: Wiley) ch 20
[25] Ruelle D 1999 *Statistical Mechanics. Rigorous Results* (Singapore: World Scientific) p 130
[26] Baxter R J 1991 *Exactly Solved Models in Statistical Physics* (London: Academic)
[27] Kierlik E, Rosinberg M L, Tarjus G and Viot P 2001 *Phys. Chem.–Chem. Phys.* at press
[28] Binder K 1981 *Z. Phys.* B **45** 61
[29] Bock H and Schoen M 2001 in preparation